The EMBO Journal vol.10 no.8 pp.1997 - 2005, 1991

The three-dimensional structure of class π glutathione S-transferase in complex with glutathione sulfonate at 2.3 Å resolution

Peter Reinemer[1], Heini W.Dirr[1,2], Rudolf Ladenstein[1], Jörg Schäffer[1], Oliver Gallay[1] and Robert Huber[1]

[1]Max Planck-Institut für Biochemie, W-8033 Martinsried bei München, FRG and [2]Department of Chemistry and Biochemistry, Rand Afrikaans University, PO Box 524, Johannesburg 2000, South Africa

Communicated by R.Huber

The three-dimensional structure of class π glutathione S-transferase from pig lung, a homodimeric enzyme, has been solved by multiple isomorphous replacement at 3 Å resolution and preliminarily refined at 2.3 Å resolution (R = 0.24). Each subunit (207 residues) is folded into two domains of different structure. Domain I (residues 1–74) consists of a central four-stranded β-sheet flanked on one side by two α-helices and on the other side, facing the solvent, by a bent, irregular helix structure. The topological pattern resembles the bacteriophage T4 thioredoxin fold, in spite of their dissimilar sequences. Domain II (residues 81–207) contains five α-helices. The dimeric molecule is globular with dimensions of about 55 Å × 52 Å × 45 Å. Between the subunits and along the local diad, is a large cavity which could possibly be involved in the transport of non-substrate ligands. The binding site of the competitive inhibitor, glutathione sulfonate, is located on domain I, and is part of a cleft formed between intrasubunit domains. Glutathione sulfonate is bound in an extended conformation through multiple interactions. Only three contact residues, namely Tyr7, Gln62 and Asp96 are conserved within the family of cytosolic glutathione S-transferases. The exact location of the binding site(s) of the electrophilic substrate is not clear. Catalytic models are discussed on the basis of the molecular structure.

Key words: crystallography/detoxification/glutathione S-transferase/intracellular transport/structure

Introduction

Glutathione S-transferases (EC 2.5.1.18) are a ubiquitous family of multifunctional proteins involved in the cellular detoxification of cytotoxic and genotoxic compounds and in protecting tissues against oxidative damage (for recent reviews see Mannervik and Danielson, 1988; Boyer, 1989; Pickett and Lu, 1989; Coles and Ketterer, 1990). They have also been implicated in the development of resistance of cells and organisms to electrophilic anticancer drugs, pesticides and herbicides (Hayes and Wolf, 1988; Waxman, 1990). Multiple drug resistance can severely limit the effectiveness of many useful chemotherapeutic agents. However, glutathione S-transferases may be useful targets for improving chemotherapy through the use of inhibitory peptide analogs of glutathione (Waxman, 1990).

As enzymes, glutathione S-transferases are versatile and catalyze the nucleophilic addition of the thiol of reduced glutathione to a wide variety of hydrophobic electrophiles including alkyl and aryl halides, epoxides, quinones and activated alkenes. The glutathionyl S-conjugates of these compounds are more polar thus facilitating their elimination. Certain transferases can also catalyze a selenium-independent peroxidase activity with lipid and nucleic acid hydroperoxides as substrates, while others catalyze the isomerization of Δ^5-3-ketosteroids, in which glutathione serves a true co-enzyme role (reviewed in Douglas, 1987; Mannervik and Danielson, 1988).

In addition to their catalytic capabilities, glutathione S-transferases also exhibit a ligand binding ('ligandin') function that can facilitate the intracellular transport of numerous hydrophobic and amphiphatic compounds such as bilirubin, heme, steroids and bile salts (Ketterer *et al.*, 1978; Listowkski *et al.*, 1988). Binding often results in the inhibition of glutathione S-transferase activity by the bound ligand.

The mammalian cytosolic glutathione S-transferases can be grouped into three species-independent classes, namely α, μ and π (Mannervik *et al.*, 1985). Multiple homodimeric and heterodimeric forms (M_r ~50 000) of the protein occur as the result of multiple genes and subunit hybridization. Although *in vitro* generated dimers of transferases between subunits from different species are possible, interclass heterodimers are not known. There is no evidence for active monomeric species. The three classes appear to constitute essentially separate and distinct enzymes, whereas the members within a class represent isozymes (Persson *et al.*, 1988).

In addition to the cytosolic enzymes, a distinct membrane-bound enzyme, referred to as microsomal glutathione S-transferase, has been identified, but shows no obvious sequence homology with any of the soluble enzymes (Morgenstern and De Pierre, 1988).

The soluble enzymes have two active sites per dimer each of which functions independently of the other (Danielson and Mannervik, 1985). Although their three-dimensional structure is not known, the active site is suggested to consist of a glutathione binding region (the G-site) and a non-specific hydrophobic region (the H-site) to accommodate the electrophilic substrates (Mannervik, 1985). A model of the G-site, based on data from kinetic studies with glutathione analogs, has been presented (Adang *et al.*, 1990).

Exactly how the protein enhances the nucleophilic reactivity of glutathione is not known, but two mechanisms have been proposed. One involves general-base catalysis while the other involves a destabilization of enzyme-bound glutathione effectively reducing the pK_a of its thiol group (Jakoby, 1978; Mannervik and Danielson, 1988) In the light of the foregoing discussion, a high resolution crystallographic investigation of the glutathione S-transferases is essential to arrive at a better and detailed understanding of their structural

and functional properties. Crystals suitable for X-ray diffraction analyses have been obtained of isozymes from class α, μ and π (Sesay *et al.*, 1987; Schäffer *et al.*, 1988; Cowan *et al.*, 1989; Parker *et al.*, 1990;. Dirr *et al.*, 1991), but no structure reported.

We describe here, for the first time, the three-dimensional structure of the class π glutathione S-transferase from pig lung and attempt to relate this to its functional properties.

Results and discussion

Overall structure of class π glutathione S-transferase

Class π glutathione S-transferase from pig lung is a dimer composed of identical subunits (Dirr *et al.*, 1991). The observed electron density is in agreement with its chemical sequence except for extension at the C terminus with four residues, NGKQ. Protein material from the same batch was used for both crystallizations and sequencing, and it is not clear why the four residues were not detected during chemical sequencing. The failure may be related to the tendency of the -N-G-structure to form an imide leading to the generation of a β-aspartyl peptide bond (Bornstein, 1970). The complete sequence is displayed in Figure 5.

The folding topology of the subunit polypeptide chain is characterized by two very different domains, one being α/β, while the other is almost all α (Figure 1a). Domain I (residues 1–74), the smaller of the two (dimensions about 29 Å × 24 Å × 23 Å), consists of a central four-stranded β-sheet showing a right-handed twist of about 45° when viewed along the strands, three α-helices, one turn of 3_{10}-helix, three β-turns and a *cis*-Pro bend (Figure 1a,b). β-Strand β2 (residues 29–32), which is at the solvent-exposed edge of the β-sheet, is aligned parallel, while the other three, β1 (residues 3–7), β3 (residues 52–55) and β4 (residues 58–61) are antiparallel. No β-bulges are present. A hairpin bend connects strands β3 and β4, while β1 and β2 are joined by a right-handed crossover connection. The latter comprises a β-turn (residues 11–14) and an α-helix, αA (residues 15–23), and is associated with that side of the β-sheet shielded from solvent. A second α-helix, αC (residues 63–74), is also situated at this side of the β-sheet. There is a hydrophobic core present between the layer of adjacent helices and the β-sheet. A bent irregular helix, αB (residues 38–43), connects β2 and β3 and interacts weakly with solvent-exposed side of the β-sheet. Its helical axis is almost perpendicular to the direction of the β-strands which is in contrast to the parallel/antiparallel arrangements often found for interactions between helices and β-sheets (Chothia *et al.*, 1977).

Despite their very different amino acid sequences, the tertiary structure of domain I resembles the general fold of thioredoxin from bacteriophage T4, which has a $\beta\alpha\beta\alpha\beta\beta\alpha$ topological pattern (Söderberg *et al.*, 1978). Related folds are also observed in thioredoxin from *Escherichia coli* (Holmgren *et al.*, 1975) and glutathione peroxidase (Ladenstein *et al.*, 1979), as displayed in Figure 1c. Whether these conformational similarities indicate structural convergence or a common evolutionary origin is not clear.

Domain II (residues 81–207) is covalently connected to domain I by a short segment (residues 75–80) with the side chain of Tyr77 wedged between αA and αC.

It comprises five α-helices, one turn of 3_{10}-helix (residues 135–137) and four β-turns (residues 140–143, 164–167, 168–171, 196–199) but no β-strands (Figure 1a). The α-helices are: αD (residues 81–107), αE (residues 109–132), αF (residues 148–163), αG (residues 172–182) and αH (residues 185–192). Helices αD, αE and αF are wound into almost one and a half turns of a right-handed superhelix. The latter is generated by the up–down arrangement of αD and αE, with their short 'S'-shaped connector, and the crossover connection (residues 134–147) between αE and αF permitting αF to pack against αD. This

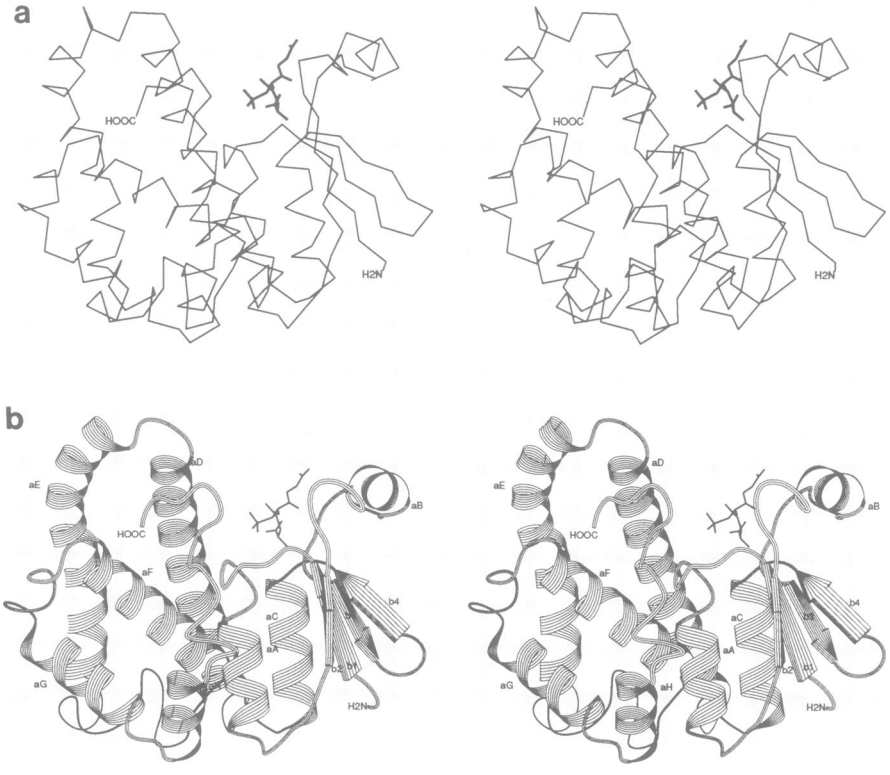

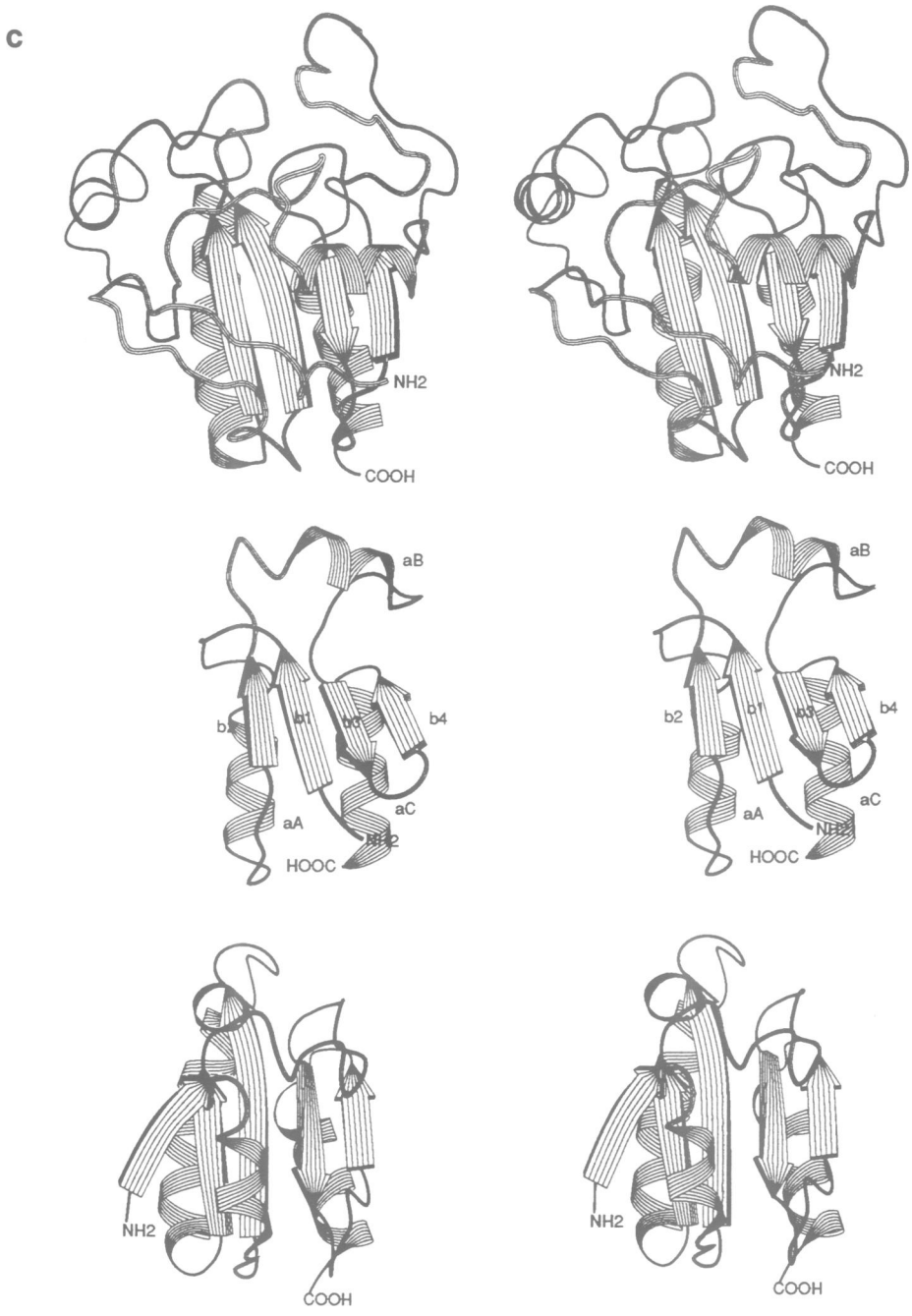

Fig. 1. (**a**) Stereo drawing showing the C^{α} positions of a subunit of glutathione S-transferase (thin line) with the model of the inhibitor glutathione sulfonate included (thick line). (**b**) Stereo-ribbon diagram (Priestle, 1988) of a subunit of glutathione S-transferase with the model of the inhibitor glutathione sulfonate included (thick line). (**c**) Stereo-ribbon diagram (Priestle, 1988) of domain I of glutathione S-transferase (**middle**) compared with glutathione peroxidase (**top**; Ladenstein *et al.*, 1979) and thioredoxin from *E.coli* (**bottom**; Holmgren *et al.*, 1975).

folding topology bears a relationship to the five-helix globule recently described for human annexin V repeats (Huber *et al.*, 1990).

The bent appearance of αE is most likely due to the effects of two Pro residues (Pro121 and Pro126) in the α-helix (Richardson and Richardson, 1990). αG is almost perpendicular to αF, with their connecting segment (residues 164−171) comprising two β-turns, packing against the N-terminal region of αE. Together, helices αD, αE, αF and αG as well as their connecting sequences form a closely packed elongated structure (dimensions about 42 Å × 26 Å × 23 Å), their path tracing a right-handed spiral. αH on the other hand, is slightly separated from this structure, but is connected to it covalently by a short segment (residues 183−184). It is also attached noncovalently through some side chains in the C-terminal end (residues 193−207) of the polypeptide chain as follows: after αH, the sequence at this end turns at Asn198 in a β-turn (residues 196−199) toward the major domain II structure, and at Ile201 it bends up then forms a loop (residues 201−207) which associates with the C- and N-terminal ends of αD and αE respectively. Side chains within hydrogen-bonding distance of each other are: Asn202 and Tyr101 (αD), Lys206 and Glu110 (αE), and Gln207 and Tyr109 (αE).

The separation of αH from the other helices in domain II creates an opening in this domain situated near the G-site in domain I and facilitating diffusion of small molecules. Non-covalent contacts between domains I and II are mediated by the main chain and side chains primarily in αA and αC, and in αD, αF and αH respectively. Most hydrophobic interactions occur where αA makes contact with αF and αH, while polar contacts form between αC and αD. Polar contacts also secure a region (residues 196–201) of the polypeptide's C-terminal end to αA as well as to Arg11 which is in a β-turn preceding αA. No disulfide bridges are observed, confirming our previous findings (Dirr *et al.*, 1991).

According to the present model, the class π subunit comprises ~56% α-helix, 3% 3_{10}-helix and 8% β-strands. Predictions of secondary structure content have not been accurate, yielding values of 36% α-helix and 22% β-sheet for the pig isozyme (H.W.Dirr, unpublished results), and 37% α-helix and 16% β-sheet for the human homolog (Ahmad *et al.*, 1990). Furthermore, predictions of alternating α-helices and β-strands along the entire polypeptide chain (Persson *et al.*, 1988; Ahmad *et al.*, 1990) are also misleading.

Dimeric glutathione S-transferase is assembled as shown in Figure 2 and has a globular shape with molecular dimensions of about 55 Å × 52 Å × 45 Å. The accessible surface area for a subunit in the dimer is 8975 $Å^2$ compared with 10345 $Å^2$ for an isolated subunit. A prominent feature in the dimeric structure is a very large cavity formed between the two subunits and whose presence here seems to explain the moderate (13%) coverage of accessible surface area upon dimerization. Large ligands could bind to this cavity, but the large number of polar residues coating it may impede interactions with highly hydrophobic compounds.

Intersubunit contacts are mediated mainly by hydrophobic residues in a β-turn (residues 45–48), strand β4 and helix αC in domain I of one subunit and the antiparallel helix pair, αD and αE, in domain II of the other subunit.

Active site and inhibitor binding

Dimeric glutathione S-transferase binds two molecules of glutathione sulfonate, a competitive inhibitor, as illustrated in Figures 1 and 2. Interpretation of well defined electron density near the side chain of Tyr7, which could not be accounted for by protein during refinement, was clear and a model of the inhibitor could be fitted reasonably well to this density (Figure 3). The conformation of the bound glutathione analog is an extended one, similar to the X-ray structure of reduced glutathione (Wright, 1958), and of glutathione bound at the active site of glutathione reductase (Karplus *et al.*, 1989), Glyoxalase I (Rosevear *et al.*, 1984) and possibly glutathione peroxidase (Epp *et al.*, 1983). The glutathione sulfonate differs from reduced glutathione by the replacement of the thiol moiety by a negatively charged sulfonate group. It is not clear at present whether the binding features of these two compounds are identical, but the specific interactions between protein and glutathione backbone atoms, as discussed below, argue against substantial differences.

Glutathione sulfonate occupies a site on domain I [hereafter referred to as the G-site after Mannervik (1985)] which is situated in a cleft formed between intrasubunit domains. The cleft extends from a segment (residues 8–10) connecting strand β1 to helix αA, to about Ser63 at the N-terminal end of helix αC. One end of the cleft opens out to bulk solvent, while the other, near Ser63, is adjacent to the cavity at the center of the dimer. Side chains lining the G-site include

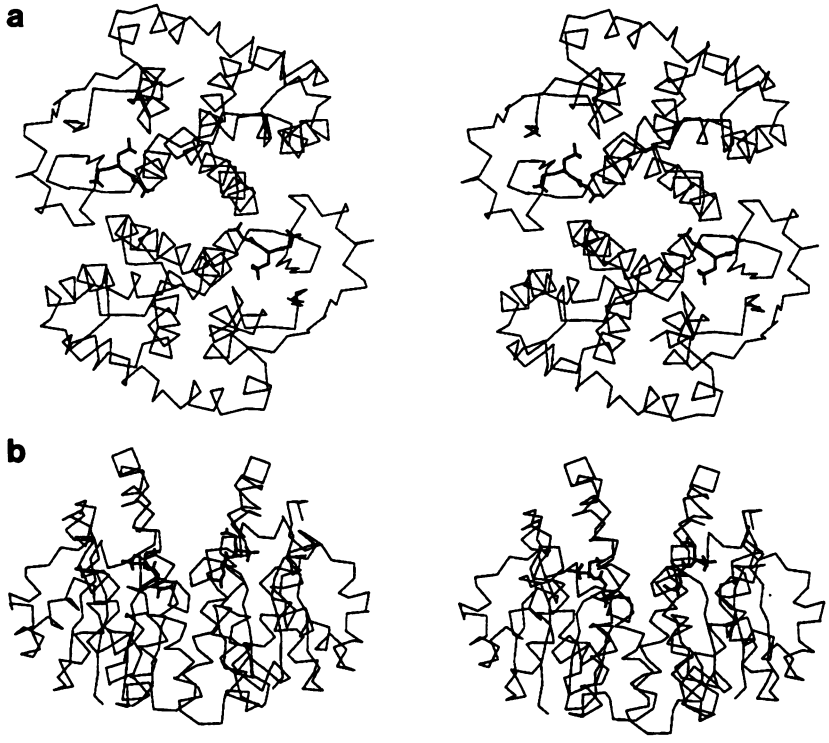

Fig. 2. Stereo drawing of the C^{α} positions of the dimeric glutathione S-transferase molecule (thin line) with the inhibitor glutathione sulfonate included (thick line). (**a**) Along the local two-fold and (**b**) perpendicular to the local two-fold.

Tyr7, Gly12, Arg13, Trp38, Lys42, Gln49, Pro51, Gln62, Ser63 and Glu95.

The enzyme bound inhibitor is accessible to solvent and orientated at the G-site with its γ-glutamyl arm pointing downward in the direction of the dimer's large cavity, while the sulfonate moiety is pointing towards domain II, and the glycine part pointing away from domain II and in the direction of bulk solvent. Inhibitor molecules occupying G-sites on neighboring subunits are separate by about 14 Å between their γ-glutamyl carboxylate groups. It seems unlikely that dimerization directly enhances the hydrophobicity at the catalytic point (Adams and Sikakana, 1990), because the sulfur atom of the bound glutathione analog is situated away from the neighboring subunit. Recognition and binding of glutathione sulfonate, and most likely the reduced form of glutathione as well, involves several side-chain and main-chain polar interactions. Those residues most likely to participate in sequestering the inhibitor at the G-site are displayed labeled in Figure 4. No water-mediated hydrogen bonding has been included at this stage of refinement. The γ-glutamyl's α-carboxyl group interacts with the side chains of Arg13 and Gln62, confirming the suggestion that an arginine residue serves as an anionic recognition site for glutathione S-transferases (Schasteen *et al.*, 1983). Furthermore, Gln62 has an unfavorable main chain conformation, suggesting that it may have to move to allow inhibitor binding. An induced conformational change in the structure would also explain the altered reactivity of Cys45 occurring upon binding glutathione analogs (Dirr *et al.*, 1991), as no cysteine residues are present in the G-site (Figure 4). Interestingly, the only residue in the neighboring subunit which might associate with enzyme bound inhibitor is Asp96. Its side chain is close to the γ-glutamyl's α-carboxylate group, the nature of the interaction not being clear at this stage as one would expect repulsion between the two carboxylates rather than attraction. Another interaction with the γ-glutamyl moiety is through its γ-carboxyl group and the side chain of Gln49.

The sulfonate group of the inhibitor interacts with the side chain of Tyr7 (Figures 3 and 4). This tyrosine residue is also fully conserved in the aligned amino acid sequences of mammalian (class α, μ and π), *Schistosoma japonicum* and maize glutathione S-transferases, but not in the sequence of the microsomal enzyme (for sequences, see Mannervik and Danielson, 1988). Tyr7 is located at a site equivalent to the active site disulfides of the thioredoxins and the seleno-cysteine of glutathione peroxidase. On the basis of this particular interaction, our model could explain the greater affinity of glutathione S-transferases for glutathione analogs, in which the cysteine has been replaced by moieties having electronegative side chains, such as carboxylates (Graminski *et al.*, 1989a; Adang *et al.*, 1991). Furthermore, binding

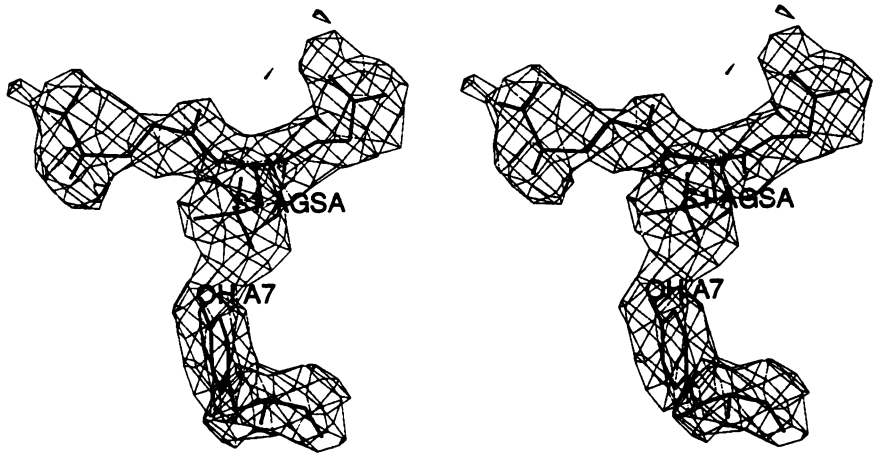

Fig. 3. Model of the inhibitor glutathione sulfonate and Tyr7 with the difference electron density ($2F_o-F_c$) calculated without inhibitor and contoured at 0.9 σ.

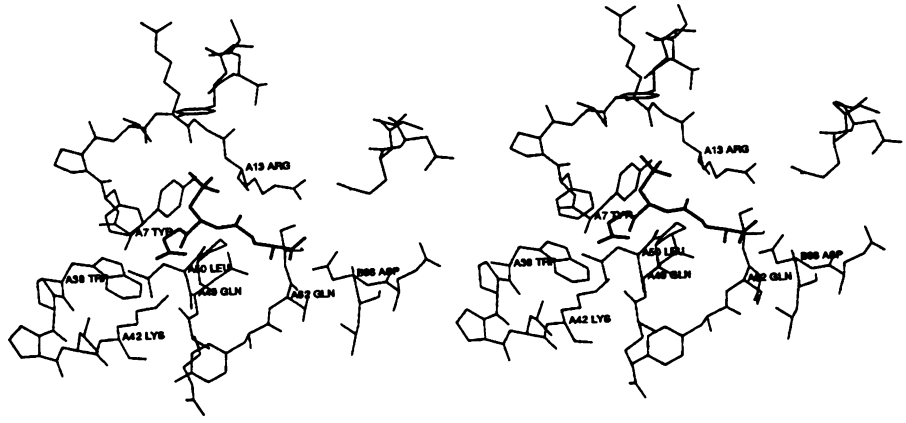

Fig. 4. Model of inhibitor glutathione sulfonate and its next neighbors at the binding site.

of these compounds was also shown to be highly stereospecific, since inhibition was strong only when the orientation of the electronegative group was the same as for the thiol group of glutathione. The tight hydrogen bonding interaction between the cysteine sulfonate and Tyr7 bears a resemblance to the bond between tyrosine sulfonate of hirudin (Tyr63) and the side chain of Tyr76 of thrombin (Grütter *et al.*, 1990; Rydel *et al.*, 1990). The α-carboxyl function of the inhibitor's glycine makes contact with the side chains of Trp38 and Lys42. Its amide nitrogen does not interact with protein as it points into the bulk solvent. Although the glycine moiety is suggested not to be as essential as the γ-glutamyl group for binding (Adang *et al.*, 1990), the presence of its α-carboxyl group will exert a stabilizing effect.

Hydrogen bonding between the main chain and both peptide bonds in glutathione sulfonate also contributes to the recognition process. A short antiparallel β-pleated sheet results from the interaction between the amide nitrogen and carbonyl oxygen of Leu50 with the inhibitor's $CySO_3^-$ carbonyl oxygen and amide nitrogen respectively. Furthermore, Pro51 in *cis*-conformation seems to be an essential element. This structural feature could also explain why N^4-(malonyl-D-cysteinyl)-L-2,4-diaminobutyrate, the retro-inverso isomer of glutathione, in which the direction of the peptide bonds is reversed, is a very poor substrate for glutathione S-transferases (Chen *et al.*, 1986). However, kinetic data (Sugimoto *et al.*, 1985) would seem to suggest that these peptide bond interactions, although important, are not essential in substrate binding, since the cysteinglycine dipeptide is not a substrate for glutathione S-transferases, whereas the γ-glutamylcysteine dipeptide is utilized to some extent. The extent to which the γ-glutamyl moiety is sequestered by protein functionalities in comparison with other moieties of the inhibitor is in accord with the proposal (Adang *et al.*, 1990) that this moiety is the principal binding determinant of glutathione and its analogs.

What is not clear from our present model is the exact location of the region (H-site) in the active site to which the electrophilic substrate binds. The H-site is proposed to be hydrophobic and must be adjacent to the G-site, and should also permit proper orientation of the bound reactants. In our model there appear to be three possible locations for this site. The first possibility is a cavity in domain II, to which the sulfur of the bound inhibitor is directed. It is formed largely as a result of the separation of the α-helix, αH, from the main structural portion of domain II, as discussed in the previous section. Side chains lining it include Gly12, Arg13, Arg98, Tyr101, Ala102, Tyr106, Val141, Asp155, Ile159, Ile201 and Asn202. Photoaffinity labeling recently identified a corresponding region of the active site of class α isozymes, presumably where the electrophilic substrate binds (Hoesch and Boyer, 1989). The second possibility is a hydrophobic region in the cleft described above and adjacent to the G-site and which could accommodate small molecules. This region is coated by the side chains of Phe8, Pro9, Val10, Met35, Tyr106, Pro200 and Gly203. The third is the cavity formed between the subunits (Figure 2a). Experiments to establish the location(s) of the H-site(s) for various electrophilic substrates are in progress. Further hints to the location of the H-site might be expected from the structure analysis of the class π glutathione S-transferase from bovine placenta which contains a bound S-hexylglutathione moiety (O.Gallay *et al.*, in preparation).

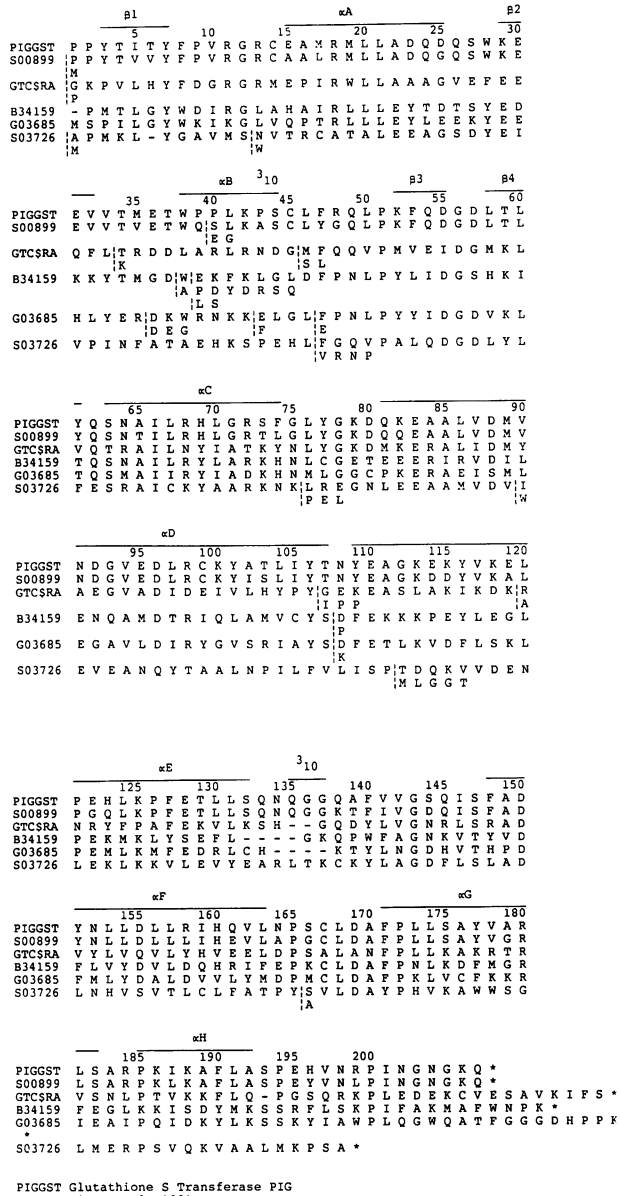

PIGGST Glutathione S Transferase PIG
Dirr et al. 1991
S00899 Glutathione transferase - Human #EC-number 2.5.1.18
Kano T., Sakai M., Muramatsu M.
Cancer Res. (1987) 47: 5626-5630
Structure and expression of a human class pi glutathione S-transferase messenger RNA.
GTCSRA GLUTATHIONE S-TRANSFERASE YC (EC 2.5.1.18) (CHAIN 2) (CLASS ALPHA)
TELAKOWSKI-HOPKINS C.A., RODKEY K.A., BENET C.D., LU A.Y.H., PICKETT C.B.;
J. BIOL. CHEM. 260:5820-5825(1985).
TU C.-P.D., LAI H.-C.J., LI N.-Q., WEISS M.J., REDDY C.C.;
J. BIOL. CHEM. 259:9434-9439(1984).
B34159 *Glutathione transferase (EC 2.5.1.18) mu2 - Mouse
Townsend, A.J., Goldsmith, M.E., Pickett, C.B., and Cowan, K.H.
J. Biol. Chem. 264, 21582-21590, 1989
Isolation, characterization, and expression in Escherichia coli of two murine mu class glutathione S-transferase cDNAs homologous to the rat subunits 3 (Yb1) and 4 (Yb2).
G03685 Schistosoma japonicum Sj26 antigen mRNA, a putative glutathione S-transferase, complete cds.
Smith D.B., Davern K.M., Board P.G., Tiu W.U., Garcia E.G., Mitchell G.F.
Proc. Natl. Acad. Sci. U.S.A. (1986) 83: 8703-8707
M-r 26,000 antigen of Schistosoma japonicum recognized by resistant WEHI 129/J mice is a parasite glutathione S-transferase.
Smith D.B., Davern K.M., Board P.G., Tiu W.U., Garcia E.G., Mitchell G.F.
Proc. Natl. Acad. Sci. U.S.A. (1987) 84: 6541-6541
S03726 Glutathione transferase I - Maize #EC-number 2.5.1.18
Shah D.M., Hironaka C.M., Wiegand R.C., Harding E.I., Krivi G.G., Tiemeier D.C.
Plant Mol. Biol. (1986) 6: 203-211
Structural analysis of a maize gene coding for glutathione-S-transferase involved in herbicide detoxification.
Wiegand R.C., Shah D.M., Mozer T.J., Harding E.I., Diaz-Collier J., Saunders C., Jaworski E.G., Tiemeier D.C.
Plant Mol. Biol. (1986) 7: 235-243
Messenger RNA encoding a glutathione-S-transferase responsible for herbicide tolerance in maize is induced in response to safener treatment.

Fig. 5. Alignment of amino acid sequences of glutathione S-transferases from pig (class π), human (class π), rat (class α), mouse (class μ), *S.japonicum* and maize. Locations of secondary structure elements along the pig sequence are indicated by $\beta 1-\beta 4$ (β-strands), $\alpha A-\alpha H$ (α-helices) and 3_{10} (3_{10}-helix).

Implications for the enzymatic mechanism

In nucleophilic catalysis, glutathione reacts predominantly as the anionic thiolate. Although most reactions catalyzed by glutathione S-transferases are nucleophilic substitutions, it is poorly understood how these enzymes exactly activate the thiol of bound glutathione and facilitate its attack on electrophiles. Essentially two mechanisms have been proposed (Jakoby, 1978; Mannervik and Danielson, 1988). In the first one, that of general base-catalysis, the protein is suggested to enhance the nucleophilicity of the thiol by providing at the active site a base of appropriate pK_a for deprotonating the thiol group. A histidine has recently been attributed this catalytic function (Awasthi *et al.*, 1987), but our model clearly shows the absence of histidine in the active site; the nearest histidine, His123 in the neighboring subunit, is about 14 Å away from the inhibitor's sulfur atom. Inactivation by chemical modification of histidine residues is therefore probably due to a conformational change of the protein. The explicit role of Tyr7 in catalysis is not clear at present, but its proximity to the glutathione sulfur suggests an important role. In the complex Tyr7 is probably protonated and neutral to allow the close association with the negatively charged sulfonate moiety of the inhibitor (Figures 3 and 4). This interaction is probably not restricted to S-sulfonates as tighter binding is observed quite generally between glutathione S-transferases and glutathione analogs with an electronegative side chain. This observation does not provide information about the pK_a of Tyr7, which might sufficiently decrease in the protein environment (see below) to act as the general base. Alternatively, the enzyme's active site could stabilize the thiolate anion of bound glutathione by effectively lowering the pK_a of its thiol moiety. Spectroscopic and kinetic data (Graminski *et al.*, 1989a,b) suggest the presence of a thiolate anion as the predominant glutathione species in binary complexes with rat glutathione S-transferases 3–3 and 4–4. The pK_a values of bound thiol, 5.7 and 6.6. respectively, are indeed much lower than the pK_a of about 9.0 (Reuben and Bruice, 1976) for glutathione in aqueous solvent. Anionic glutathione could then also, like glutathione sulfonate, interact via hydrogen bonding with Tyr7. The active site may contribute by its electrostatic potential to a reduction in pK_a of both thiol and tyrosine groups. In this respect, it is interesting to note that the N termini of the two parallel helices, αA and αC in domain I, are close to the G-site, where they may generate a positive electrostatic potential. The sulfur atom of the bound inhibitor is almost on the helix axis of αA (Figure 2). The electrostatic field could also facilitate the attraction and proper orientation of the negatively charged glutathione to the G-site approaching from solvent (Hol, 1985).

Clearly, further experimental work is needed to gain a detailed understanding of both the structural and chemical events leading up to catalysis and to the exploitation of local structures to facilitate the release of product.

Implications for other glutathione S-transferases

Amino acid sequences of four class π isoenzymes have been established (Suguoka *et al.*, 1985; Kano *et al.*, 1987; Gallay, 1990; Dirr *et al.*, 1991). On a one-to-one basis, the extent of positional identities between the pig isozyme and the other isozyme ranges over 82 to 85%, while 76% of all residues in this class are fully conserved. This clearly indicates a substantial structural relationship with the pig isozyme. In particular all residues forming G-site ligands and the complementary surface for the glutathione analog are

Table I. Statistics of diffraction data

Derivative[a]	Measurements					
	Total	Independent	Completeness[b]	R_M[c]	R_{FM}[c]	
Native	113811	22394	0.92	0.66	0.084	0.037
HACY	100909	17191	0.95	0.86	0.146	0.064
UOSO	121747	20573	0.96	0.88	0.117	0.048
NAWO	56228	14493	0.84	0.53	0.106	0.054
WOS3	103373	17601	0.97	0.93	0.096	0.037

[a]HACY: $C(HgOOCCH_3)_4$ (8.6 mg/ml) and $H_2N(CH_2)_2SH$ (4.7 mg/ml), 48 h soak. UOSO: $UO_2SO_4 \times 3\ H_2O$, 0.6 mM, 16 h soak. NAWO: Na_2WO_4, 15 mM, 46 h soak. WOS3: Cs_2WOS_3, 10 mM, 47 h soak. All compounds were dissolved in 25% (m/v) polyethylene glycol 4000, 50 mM MES/NeOH, 1 mM glutathione sulfonate, 0.02% NaN_3, pH 6.5.

[b]Completeness of data above 2.5 σ: first column ∞–2.3 Å for native and ∞–2.59 Å for derivatives; second column 2.38–2.3 Å for native and 2.73–2.59 Å for derivatives.

[c]R_M: $\Sigma(I - <I>)/\Sigma I$, for all measurements. R_{FM}: $\Sigma(I_F - <I_F>)/\Sigma I_F$, where I_F is the averaged value of point group related reflections, $<I_F>$ is the averaged value of a Bijvoet pair.

Table II. Heavy atom parameters

Occ	X	Y	Z	B_{11}	B_{12}	B_{13}	B_{22}	B_{23}	B_{33}
HACY	F_H/Res 2.43								
70.19	0.5382	0.0595	0.4926	0.00074	0.00038	−0.00034	0.00108	0.00093	0.00218
73.11	0.6333	0.5298	0.3148	0.00073	0.00059	0.00030	0.00084	0.00061	0.00075
48.28	0.6598	0.3238	0.0185	0.00069	−0.00016	−0.00038	0.00118	−0.00013	0.00203
22.01	0.3863	0.2512	0.5296	0.00077	−0.00139	−0.00068	0.00302	0.00154	0.00355
UOSO	F_H/Res 0.43								
16.45	0.5480	0.4310	0.1981	0.00044	0.00033	0.00048	0.00114	−0.00111	0.00190
11.96	0.4765	0.1488	0.3407	0.00104	−0.00132	0.00088	0.00235	−0.00053	0.00286
NAWO	F_H/Res 0.43								
24.51	0.3618	0.4097	0.9527	0.00055	−0.00094	0.00133	0.00192	−0.00046	0.00526
WOS3	F_H/Res 0.27								
10.02	0.3598	0.4085	0.9548	0.00052	−0.00006	0.00093	0.00126	−0.00060	0.00127

Figure of merit 25.0–3.0 Å: 0.74

Occ: occupancy in relative units. X, Y, Z: fractional coordinates. $B_{11}-B_{13}$: anisotropic temperature parameters. F_H/Res: r.m.s. mean heavy atom contribution/r.m.s. residual, defined as $[(F_{PHC}-F_{PH})^2/n]^{1/2}$ with the sum over all reflections, where F_{PHC} is the calculated structure factor of the heavy atom derivative and F_{PH} is the structure factor amplitude of the heavy atom derivative.

invariant. Residue differences occur at 51 positions and relating these substitutions to the three-dimensional structure of the pig isozyme shows that ~35 of them (at positions 6, 25, 34–37, 39, 40, 43, 44, 54, 73, 82, 102, 103, 111, 114, 115, 119, 123, 132, 138, 144, 158, 161, 164, 166, 170, 179–182, 192 and 195) are at the surface of the molecule. Few, if any, of the differences involving inter-subunit contacts (at positions 47, 48, 65, 82 and 122) can be of major importance, since hybrid dimers can be formed *in vitro* between the subunits of different species (Mannervik and Danielson, 1988). The contacts at the interdomain area are largely conserved, and the nature of most substitutions there (at positions 11, 15, 25, 74, 196, 197 and 199) should not incur major changes. Furthermore, only three substitutions are in totally internal regions (at positions 5, 17 and 141) suggesting that the hydrophobic cores, and hence the overall packing geometry, are largely preserved. It seems, therefore, that the amino acid differences observed between class π isozymes could be accommodated reasonably well in conserved three-dimensional structures.

Differences in catalytic turnovers between the π isozymes (Mannervik and Danielson, 1988; Schäffer *et al.*, 1989; Dirr *et al.*, 1991) are most likely related to structural differences induced by some of the substitutions. As soon as the three-dimensional structures of other class π isozymes become available a direct and more meaningful comparison between structures will be possible. It should also become clear how the other isozymes accommodate an extra two residues which are inserted between positions 39 and 40 in αB.

Although the glutathione S-transferases belong to a common family of functionally related molecules, the structural relationship between the isozyme from class π and the isozymes from class α and class μ are not obvious from their primary structures. Positional identities between the pig isozyme and individual members of the other two classes do not exceed 34% (Mannervik and Danielson, 1988; Persson *et al.*, 1988; Dirr *et al.*, 1991). Moreover, ~23 residues are fully conserved throughout all classes of mammalian species, of which five—Tyr7, Gln(Asn)49, Pro51, Gln62 and Asp86—are G-site residues. Many replacements are conservative. This is valid also for the *S.japonicum* and the maize enzymes (Figure 5). Although the various isozymes obviously share a common fold, slight structural differences between their G-sites could explain the differences observed in the degrees of response of isozymes from different classes toward modifications in the glutathione molecule (Adang *et al.*, 1990, 1991). Specificity differences toward the electrophilic substrate are also most likely to be correlated to structural differences between their H-sites.

Table III. Transformation of monomer B to A

Matrix	−0.00290	0.00930	0.99995	Rotation in polar
	0.01461	−0.99985	0.00934	coordinates: ψ: 89.5°,
	0.99989	0.01464	0.00277	ϕ: −45.1°, χ: 179.8°
Vector	37.21112	47.55793	−37.70663	

Table IV. Course of refinement

Round	Resolution (Å)	Cycle	Energy (kcal/mol)	Wd (Å)	Wa (°)	R (%)
1	8–2.8	0	−398.9			48.7
		6	−939.3	0.016	2.8	37.0
2	8–2.5	0	−1588.1			43.1
		11	−1874.1	0.011	2.3	30.0
3	8–2.5	0	−1980.2			39.3
		11	−2237.7	0.009	2.1	27.0
4	8–2.3	0	−2424.8			38.9
		10	−2506.0	0.008	1.9	26.2
5	8–2.3	0	−2588.7			28.1
		10	−2794.7	0.006	1.6	24.1

Wd: mean deviation of bond length from target values. Wa: mean deviation of bond angles from target values.

Materials and methods

Purification and crystallization of glutathione S-transferase from pig lung

Class π glutathione S-transferase was prepared and crystallized as described by Dirr *et al.* (1991). Briefly, fresh pig lungs were homogenized and extracted with a dithiothreitol-containing extraction buffer. A cytosol fraction was prepared and subjected to affinity chromatography on S-hexylglutathione Sepharose as described by Mannervik and Guthenberg (1981). Fractions containing enzyme activity were pooled and further purified to apparent homogeneity by anion exchange chromatography on DEAE cellulose. Crystallizations were performed at 22°C. Hanging droplets were made by mixing 3 μl protein solution (15–20 mg/ml protein in 10 mM MES/NaOH buffer, 0.02% NaN_3, pH 6.5), 1 μl glutathione sulfonate solution (18 mM glutathione sulfonate in 50 mM MES/NaOH, 0.02% NaN_3, pH 6.5) and 2 μl precipitating buffer. The enzyme was crystallized by vapor diffusion against 16% (m/v) polyethylene glycol 4000 in 50 mM MES/NaOH, 0.02% NaN_3, pH 6.5. Crystals were obtained after ~5 days. Sometimes, crystal growth had to be initiated by seeding the droplets after ~36 h with microcrystals grown under identical conditions. They were harvested into 25% (m/v) polyethylene glycol 4000 in 50 mM MES/NaOH, 1 mM glutathione sulfonate, 0.02% NaN_3, pH 6.5, and diffract to at least 2.1 Å resolution. The crytals were orthorhombic and belong to the space group $P2_12_12_1$ with lattice constants a = 101.25 Å, b = 82.53 Å, c = 54.28 Å, $\alpha = \beta = \gamma = 90°$. The asymmetric unit contains a dimer.

Structure analysis

All X-ray measurements were done on a FAST television area detector diffractometer (Enraf-Nonius, Delft) mounted on a Rigaku rotating anode X-ray generator operated with a copper target at 5.4 kW with an apparent 0.3 × 0.3 focal spot. X-ray intensities were evaluated with the MADNES system (Messerschmidt and Pflugrath, 1987) and scaled, corrected for absorption effects and averaged (Messerschmidt *et al.*, 1990). Data collection statistics are given in Table I.

Local symmetry elements in the Patterson function were analyzed with the rotation function operated in direct space (Huber, 1965) as implemented in the PROTEIN program package (Steigemann, 1974). A preliminary orientation for a non-crystallographic 2-fold symmetery axis was obtained.

Heavy atom derivatives were prepared by soaking under the conditions given in Table II and were analyzed by difference Patterson methods using PROTEIN. The first derivative, prepared from a mixture of tetrakis-(mercury-acetoxy)methane and cysteamine (Hoeffken *et al.*, 1988), was interpreted with two pairs of local symmetry related binding sites. The correct handedness of the heavy atom structure was determined by single isomorphous replacement and solvent flattening (Wang, 1985). Several other derivatives were prepared and analyzed by difference Fourier and difference Patterson techniques, but most of them turned out to be uninterpretable due to nonisomorphism or to other reasons. Reliable derivatives were included in phase calculation and parameter refinement. A Fourier map calculated at 3 Å resolution was very noisy, but showed secondary structure elements and became interpretable in terms of the sequence after averaging the densities of the two independent monomers using the program system MAIN (D.Turk, unpublished). The symmetry relation between them was determined from related heavy atom binding sites and improved by picking 1116 density peaks above 1σ around the center of the dimer and searching for the optimal correlation with (local) symmetry related density points by alternate three-dimensional rotation and translation grid searches. The final orientation was determined by a least squares fit of subunit B to subunit A. The transformation between monomers A and B is given in Table III. It corresponds to an almost perfect 2-fold rotation around an axis lying nearly in the (x,z)-plane (inclination against y: 89.5°) at an angle of −45.1° to the x-axis. The rotation angle is 179.8° with a screw component of −0.02 Å.

A model of the polypeptide chain was built for residues 1–207 with the interactive graphics program FRODO (Jones, 1978). Although residues

204–207 are not present in the chemical sequence (Dirr *et al.*, 1991), they are unambiguously defined in the electron density map and were incorporated in the molecular model. Furthermore, identification of the added inhibitor, glutathione sulfonate, in the electron density map was easily possible.

The model was refined in five rounds using EREF (Jack and Levitt, 1978) as described in Table IV. After each round a phase-combined Fourier map was calculated and the model checked and rebuilt; resolution was extended from 3.0 Å to 2.3 Å during the refinement procedure. Solvent was not included at this stage. The preliminarily refined model, on which interpretation is based, has an R-factor of 24.1% from 9 to 2.3 Å resolution.

Acknowledgements

We thank M.Schneider for excellent assistance with some of the computations, and Dr M.T.Stubbs for some helpful suggestions on scientific matters. We are grateful to a referee who suggested a possible reason for the sequencing problem at the N–G bond. The support by the Deutsche Forschungsgemeinschaft to P.R., R.L., J.S. and R.H., and by the Foundation for Research Development and Alexander-von-Humboldt Stiftung to H.W.D. are gratefully acknowledged.

References

Adams,P.A. and Sikakana,C.N.T. (1990) *Biochem. Pharmacol.*, **39**, 1883–1889.

Adang,A.E.P., Brussee,J., Meyer,D.J., Coles,B., Ketterer,B., Van Der Gen,A. and Mulder,G.J. (1988) *Biochem. J.*, **255**, 721–724.

Adang,A.E.P., Meyer,D.J,. Brussee,J, Van Der Gen,A., Ketterer,B. and Mulder,G.J. (1989) *Biochem. J.*, **264**, 759–764.

Adang,A.E.P., Brussee,J., Van Der Gen,A. and Mulder,G.J. (1990) *Biochem. J.*, **269**, 47–54.

Adang,A.E.P., Brussee,J., van der Gen,A. and Mulder,G.J. (1991) *J. Biol. Chem.*, **266**, 830–836.

Ahmad,H., Wilson,D.E., Fritz,R.R., Singh,S., Medh,R.D., Nagle,G.T., Awasthi,Y.C. and Kurosky,A. (1990) *Arch. Biochem. Biophys.*, **278**, 398–408.

Awasthi,Y.C., Bhatnagar,A. and Singh,S.V. (1987) *Biochem. Biophys. Res. Commun.*, **143**, 965–970.

Bornstein,P. (1970) *Biochemistry*, **9**, 2408–2421.

Boyer,T.D. (1988) *Hepatology*, **9**, 486–496.

Chen,W.-J., Lee,D.Y. and Armstrong,R.N. (1986) *J. Org. Chem.*, **51**, 2848–2850.

Chen,W.-J., Graminski,G.F. and Armstrong,R.N. (1988) *Biochemistry*, **27**, 647–654.

Chothia,C., Levitt,M. and Richardson,D. (1977) *Proc. Natl. Acad. Sci. USA*, **74**, 4130–4134.

Coles,B. and Ketterer,B. (1990) *CRC Crit. Rev. Biochem.*, **25**, 47–70.

Cowan,S.W., Bergfors,T., Jones,T.A., Tibbelin,G., Olin,B., Board,P.G. and Mannervik,B. (1989) *J. Mol. Biol.*, **208**, 369–370.

Danielson,U.H. and Mannervik,B. (1985) *Biochem. J.*, **231**, 263–267.

Dirr,H.W., Mann,K.-H., Huber,R., Ladenstein,R. and Reinemer,P. (1991) *Eur. J. Biochem.*, **196**, 693–698.

Douglas,K.T. (1987) *Adv. Enzymol.*, **59**, 103–166.

Epp,O., Ladenstein,R. and Wendel,A. (1983) *Eur. J. Biochem.*, **133**, 51–69.

Gallay,O. (1990) *Ph.D. Thesis*, Ludwig-Maximilians-Universität, München.

Graminski,G.F., Kubo,Y. and Armstrong,R.N. (1989a) *Biochemistry*, **28**, 3562–3568.

Graminski,G.F., Zhang,P., Sesay,M.A., Ammon,H.L. and Armstrong, R.N. (1989b) *Biochemistry*, **28**, 6252–6258.

Grütter,M.G., Priestle,J.P., Rahuel,J., Grossenbacher,H., Bode,W., Hofsteenga,J. and Stone,S.R. (1990) *EMBO J.*, **9**, 2361–2365.

Hayes,J.D. and Wolf,C.R. (1988) In Sies,H. and Ketterer,B. (eds), *Glutathione Conjugation: Mechanisms and Biological Significance*. Academic Press, London, pp. 316–356.

Hoeffken,H.W., Knof,S.H., Bartlett,P.A., Huber,R., Moellering,H. and Schuhmacher,G. (1988) *J. Mol. Biol.*, **204**, 417–433.

Hoesch,R.M. and Boyer,T.D. (1989) *J. Biol. Chem.*, **264**, 17712–17717.

Hol,W.G.J. (1985) *Prog. Biophys. Mol. Biol.*, **45**, 149–195.

Holmgren,A., Söderberg,B.-O., Eklund,H. and Bränden,C.-I. (1975) *Proc. Natl. Acad. Sci. USA*, **72**, 2305–2309.

Huber,R. (1965) *Acta Crystallogr.*, **19**, 353–356.

Huber,R., Römisch,J. and Paques,E-P. (1990) *EMBO J.*, **9**, 3867–3874.

Jack,A. and Levitt,M. (1978) *Acta Crystallogr.*, **A34**, 931–935.

Jakoby,W.B. (1978) *Adv. Enzymol.*, **46**, 383–414.

Jones,T.A. (1978) *J. Appl. Crystallogr.*, **11**, 268–272.

Kano,T., Sakai,M. and Muramatsu,M. (1987) *Cancer Res.*, **47**, 5626–5630.

Karplus,P.A., Pai,E.F. and Schulz,G.E. (1989) *Eur. J. Biochem.*, **178**, 693–703.

Ketterer,B., Carne,T. and Tipping,E. (1978) In Blauer,G. and Sund,H. (eds), *Transport by Proteins*. de Gruyter, Berlin, pp. 79–94.

Ladenstein,R., Epp,O., Bartels,K., Jones,A., Huber,R. and Wendel,A. (1979) *J. Mol. Biol.*, **134**, 199–218.

Listowski,I., Abramovitz,M., Homma,H. and Niitsu,Y. (1988) *Drug. Metab. Rev.*, **19**, 305–318.

Mannervik,B. (1985) *Adv. Enzymol.*, **57**, 357–417.

Mannervik,B. and Guthenberg,C. (1981) *Methods Enzymol.*, **77**, 231–235.

Mannervik,B. and Danielson,U.H. (1988) *CRC Crit. Rev. Biochem.*, **23**, 283–337.

Mannervik,B., Alin,P., Guthenberg,C., Jensson,H., Tahir,M.K., Warholm,M. and Jörnvall,H. (1985) *Proc. Natl. Acad. Sci. USA*, **82**, 7202–7206.

Messerschmidt,A. and Pflugrath,J.W. (1987) *J. Appl. Crystallogr.*, **20**, 306–315.

Messerschmidt,A., Schneider,M. and Huber,R. (1990) *J. Appl. Crystallogr.*, **23**, 436–439.

Morgenstern,R. and De Pierre,J.W. (1988) In Sies,H. and Ketterer,B. (eds), *Glutathione Conjugation: Mechanisms and Biological Significance*. Academic Press, London, pp. 157–174.

Parker,M.W., Lo Bello,M. and Federici,G. (1990) *J. Mol. Biol.*, **213**, 221–222.

Persson,B., Jörnvall,H., Alin,P. and Mannervik,B. (1988) *Protein Seq. Data Anal.*, **1**, 183–186.

Pickett,C.B. and Lu,A.Y.H. (1989) *Annu. Rev. Biochem.*, **58**, 734–764.

Priestle,J.P. (1988) *J. Appl. Crystallogr.*, **21**, 572–576.

Reuben,D.M. and Bruice,T.C. (1976) *J. Am. Chem. Soc.*, **98**, 114–121.

Richardson,J.S. and Richardson,D.C. (1990) In Fasman,G.D. (ed.), *Prediction of Protein Structure and the Principles of Protein Conformation*. Plenum Press, London, pp. 1–98.

Rosevear,P.R., Sellin,S., Mannervik,B., Kuntz,I.D. and Mildvan,A.S. (1984) *J. Biol. Chem.*, **259**, 11436–11447.

Rydel,T.J., Ravichandran,K.G., Tulinsky,A., Bode,W., Huber,R., Roitsch,C. and Fenton,J.W., II (1990) *Science*, **249**, 277–280.

Schäffer,J., Gallay,O. and Ladenstein,R. (1988) *J. Biol. Chem.*, **263**, 17405–17411.

Schasteen,C.S., Krivak,B.M. and Reed,D.J. (1983) *Fed. Proc. Am. Soc. Exp. Biol.*, **42**, 2036.

Sesay,M.A., Ammon,H.L. and Armstrong,R.N. (1987) *J. Mol. Biol.*, **197**, 377–378.

Söderberg,B.-O., Sjöberg,B.-M., Sonnerstam,U. and Bränden,C.-I. (1978) *Proc. Natl. Acad. Sci. USA*, **75**, 5827–5830.

Steigemann,W. (1974) *Ph.D. Thesis*, Technische Universität, München.

Sugimoto,M., Kuhlen-Kamp,J., Ookhtens,M., Aw,T.Y., Reeve,J., Jr and Kaplowitz,N. (1985) *Biochem. Pharmacol.*, **34**, 3643–3647.

Suguoka,Y., Kano,T., Okuda,A., Sakai,M., Kitagawa,T. and Muramatsu,M. (1985) *Nucleic Acids Res.*, **13**, 6049–6057.

Wang,B.C. (1985) *Methods Enzymol.*, **115**, 90–117.

Waxman,D.J. (1990) *Cancer Res.*, **50**, 6449–6454.

Wright,W.B. (1985) *Acta Crystallogr.*, **11**, 632–642.

Received on March 4, 1991; revised on April 22, 1991